Mechanical response of Inconel TPMS under dynamic loadings

Paul Jabin Echeveste, Louise Le Barbenchon, Philippe Viot, Aitzol Lamikiz

DYMAT TM 2022
Conference Proceedings

Mechanical response of Inconel TPMS under dynamic loadings

P. Jabin Echeveste[1]* | P. Viot PhD[1]* | Aitzol Lamikiz Mentxaka PhD[2]* | L. Le Barbenchon PhD[1]*

[1]I2M Bordeaux UMR CNRS 5295, University of Bordeaux, Arts et Metiers Institute of Technology, Bordeaux INP, INRAe, Talence, 33400, France

[2]Dept. of Mechanical Engineering , Univ. of Basque Country UPV/EHU, Bilbao, Spain

Correspondence
Louise Le Barbenchon PhD, I2M Bordeaux UMR CNRS 5295, University of Bordeaux, Arts et Metiers Institute of Technology, Bordeaux INP, INRAe, Talence, 33400, France
Email: louise.le_barbenchon@ensam.eu

Funding information
The authors thank the Euskampus-Bordeaux program for its financial support.

For this study, three classical geometries of TPMS obtained by additive manufacturing were considered. The constitutive material is an Inconel 718 alloy and the samples have a relative density around 30%. The mechanical behaviour of these structures is studied under uniaxial compression by imposing quasi-static and dynamic loadings. Taking into account the relative density, the sheet gyroid presented higher material parameters (stiffness, Specific absorbed energy, ...) because of its more generalized plastic deformation. The plateau stress of the architectured material increased by about 56 % when increasing the strain rate from 10^{-2}/s to 10^{3}/s for the skeletal gyroid.

* PJE fabricated and prepared the samples with support from ALM. PJE and LLB carried out the mechanical testing analysed the results with support from PV. LLB wrote the manuscript with support from PV. LLB, PV and ALM conceived the original idea and supervised the project.

1 | INTRODUCTION

Architectural materials allow the development of lightweight mechanical structures by optimizing the path of forces in normal or standard use [1, 2]. These structures can be used as energy absorbers since their mechanical response is often characterized by a threshold force over a long range of deformation. It is thus important to consider their behaviour under severe loadings in the case of dynamic charge (crash, shock) inducing large deformations [3, 4] according to the geometry of the structure, the constitutive material, the manufacturing process … TPMS structures were reported to exhibit enhanced mechanical properties compared with the truss-lattices at similar densities. In dynamic, the mechanical behaviour of stainless steel architectured samples has been already broadly studied [5, 6, 7, 8] in opposition to Inconel-based TPMS while Inconel is usually used for low and high temperature applications were dynamic loadings can happen.

2 | MATERIALS AND METHODS

2.1 | Samples conception and fabrication

Triply Periodic Minimal Surface (TPMS) samples were conceived thanks to the MSLattice software [9]. Three different geometries were chosen: primitive (also know as Schwarz P structure), sheet gyroid and skeletal gyroid (fig. 1). A relative density of 30% was set on MSLattice with a unit cell of 4 mm. Two different sample size were defined. One has 5×5×5 cell and the other has 3×3×3.

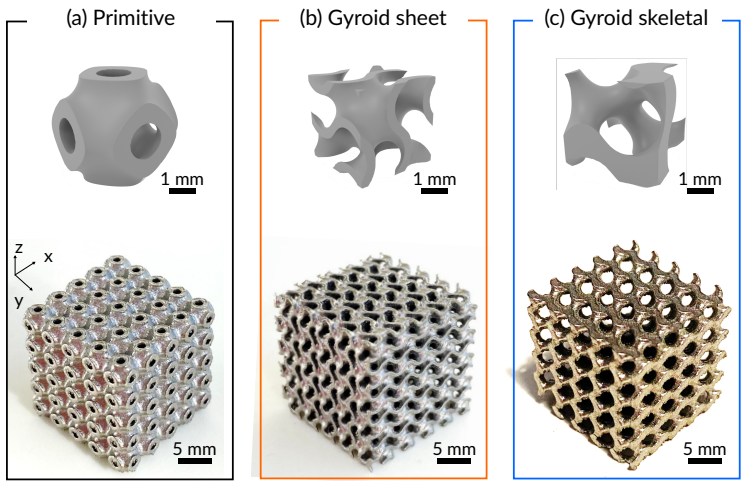

FIGURE 1 CAO of the unit cell and the resulting 5×5×5 sample. (a) Primitive. (b) Gyroid sheet. (c) Gyroid skeletal.

The samples were fabricated by additive manufacturing using the LPBF process on a Renishaw AM 500S (Bilbao, Spain). The base material an Inconel 718 alloy (ρ_{bulk} = 8190 $kg\ m^{-3}$).

The parts are manufactured in a pressure controlled chamber with a very low oxygen content which is replaced by argon. The laser has a power of 200 W, a melting point of 80 μm and a passage

speed of 2 m/s. Each layer of powders is 60 μm thick. The parts are arranged in a circular pattern and the supports between the tray and the samples are 5 mm high. For the filling of these cubes a default strategy is used. For each layer, the laser will pass twice along the contour and fill the inside with hatches (fig. 2).

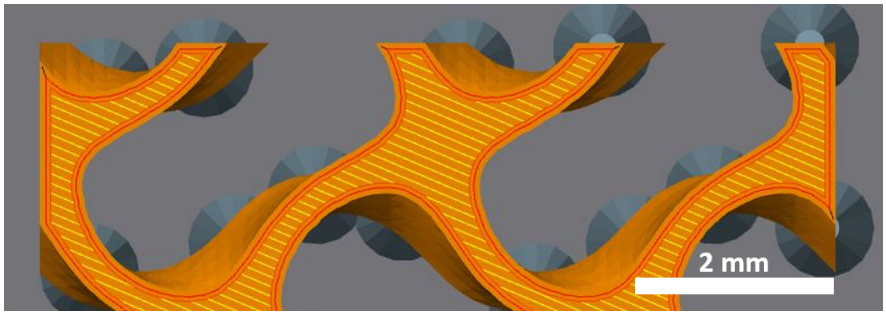

FIGURE 2 Laser path in a gyroid sheet stl cut in the slicer QuantAM.

The dimensions and mass of the resulting samples shown in fig. 1 can be found in tab. 1. Even if the CAD had the same density, it can be noticed that the resulting relative density varies depending on the geometry (tab. 1). The gyroid sheet has the highest one (0.35 ± 0.01) and the primitive has the lowest one (0.32 ± 0.01).

Geometry	Sample side length (mm)	Mass (g)	Relative density (-)
Primitive	20.3 ± 0.1	60	0.34 ± 0.01
Gyroid sheet	20.2 ± 0.2	60	0.35 ± 0.01
Gyrid skeletal	20.2 ± 0.1	60	0.32 ± 0.01

TABLE 1 Dimension and mass of the resulting TPMS Inconel cubic samples with 5×5×5 cells units obtained by additive manufacturing.

2.2 | Mechanical testing

Quasi-static compression tests were run on a Zwick Roell with a 200 kN force sensor. The displacement rate was set to 10 mm/min corresponding to a macroscopic strain rate of 8 10^{-3} s^{-1}. A camera was used to observe the deformation modes of the different samples. The acquisition frequency was set to 1 Hz.

For dynamic loadings, steel Split Hopkinson Pressure Bars (SHPB) were used to impose a compressive loading. All the bars are made of hardened maraging steel and have a diameter of 20 mm. The input, output and stricker bar lenght are respectively L_in = 3.00 m, L_out = 2.53 m and L_st = 0.50 m. One strain gauge is located on the input bar at 2.19 m from the specimen, while another is located on the output bar at 0.72 m from the specimen. Standard formulas for the wave transport are employed

to determine the force history at the output bar-specimen interface and the relative displacement of the specimen-bar interface [10]. A high speed camera (TMX phantom) was used to be able to capture local phenomenon.

From the force F and displacement Δh data, the nominal stress F/S_0 and the true strain $\ln(1+\Delta h/h_0)$ have been calculated with S_0, the initial section and h_0 the initial height of the sample. The Young's modulus E has then be calculated by fitting a first degree polynom on the elastic linear part, between a 0 strain and 0.01. Another first degree polynom was fitted between a strain of 0.05 and 0.2 to capture the plateau modulus E_p. The plateau stress σ_y is defined as the matching stress of the strain where E and E_p cross.

The specific energy absorption (SEA) was calculated until a true strain of 0.3 and is defined in compression as

$$SEA = \frac{1}{\rho_{bulk}} \int_0^{0.3} \sigma(\varepsilon) d\varepsilon. \tag{1}$$

3 | RESULTS AND DISCUSSION

Fig. 3 plots the experimental stress-strain curves under quasi-static loading. The usual three stages in cellular materials can be observed. The three geometries demonstrate first a linear elastic stage followed by a stress plateau that is more or less flat depending on the geometry.

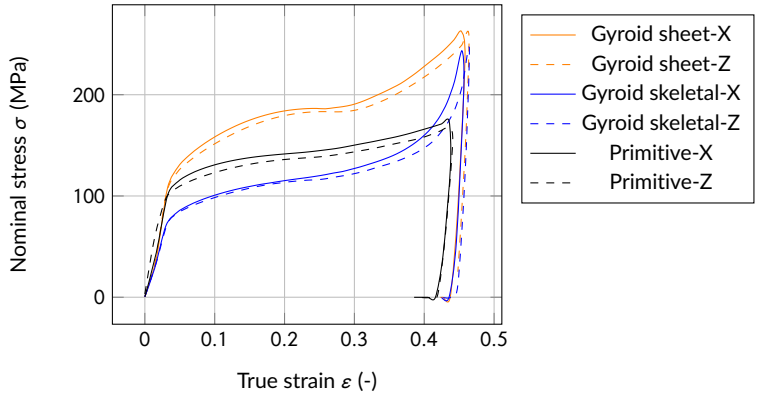

FIGURE 3 Experimental results of quasi-static compressive tests on Inconel 718 based TMPS structures.

For the skeletal gyroid geometry, the maximal displacement was enough to reach the densification stage (around 0.4) while it only starts later for the two other geometries. Macroscopically, the mechanical behaviour of the two gyroid geometries in compression seems almost isotropic (fig. 3). This observation is confirmed by the quantitative measurement of the material parameters (tab.2). For the primitive geometrie, while almost all the material parameters are isotropic, the Young's modulus is higher when the sample is loaded in the X-direction (tab. 2).

This difference in isotropy between geometries most likely comes from the specific microstructure of each geometry due to the additive manufacturing process and its interaction with the local

stress and strain fields [4]. Specific measurement of the grain orientation in the cell walls will be carried out in the future to confirm this hypothesis.

Geometry	E (GPa)	σ_y (MPa)	E_p (MPa)	SEA (J/g)
Primitive X	4.60 ± 0.27	128.1 ± 4.2	80 ± 6	7.27 ± 0.29
Primitive Z	3.23 ± 0.05	124.2 ± 4.6	93 ± 11	7.35 ± 0.21
Gyroid sheet X	4.76 ± 0.17	161.6 ± 2.7	137 ± 7	9.67 ± 0.13
Gyroid sheet Z	4.70 ± 0.40	151.6 ± 0.5	151 ± 4	9.56 ± 0.02
Gyroid skeletal X	3.17 ± 0.11	96.2 ± 0.1	117 ± 1	5.25 ± 0.03
Gyroid skeletal Z	2.90 ± 0.56	96.8 ± 0.9	103 ± 2	5.31 ± 0.01

TABLE 2 Material parameters obtained from quasi-static loading on Inconel TPMS obtained by additive manufacturing.

The material parameters are higher for the gyroid sheet geometry. Although the relative density of this geometry is greater, it is not sufficient to explain the stiffness difference and literrature confirms that the geometry of the architecture causes this enhancement [11]. The SEA, which is a linear function of the relative density [4] is also greater for the gyroid sheet geometry (9.6 J/g against 5.3 J/g for the gyroid skeletal geometry). The primitive geometry has mechanical properties (E, σ_y and SEA) between the two gyroid geometries. One can notice the the primitive geometry display the flattest plateau phase between the three TPMS structures (tab. 2).

In quasi-static, localization bands oriented at 45° can be observed for the primitive geometry (fig. 4(a)). This type of localisation is typical of periodic architectured materials [4, 12, 13]. In this structure, plastic hinges appear while the shell like structure is compressed, forming nodes. The plastic hinges of neighboring nodes interact with each other, thereby creating a continuous zone of plastic deformation. Sheet gyroids fail in a homogenous manner and all layers display relatively uniform deformations (fig. 4(a)), however previous have already show that metallic sheet gyroid mostly display the appearance of a large number of plastic hinges in the whole structure [14]. In skeletal gyroid, large rotations appear at the junction of two unit cell as the TPMS structure is compressed. It is where most plastic deformation is concentrated while the strut intersections seem to behave like rigid nodes. Instead of deforming, the latter undergo large rigid body rotations. In short, the main parameter that seems to influence the post-yield macroscopic mechanical behaviour and the material parameters of the TPMS is the ability of the structure to develop plasticity inside.

The resulting stress/strain data obtained in the dynamic regime with the steel SHPB are noisy (fig. 5). The experimental set-up needs to be improved in order to draw conclusions on the effect of the strain-rate on the mechanical behaviour of those Inconel-based TPMS. One can yet notice that the plateau stress is enhanced by the strain-rate (fig. 5). From 96 MPa for the skeletal gyroid loaded in the X-direction in quasi-static, it goes up to about 150 MPa in dynamic. According to other studies on metallic TPMS (stainless steel), this effect is due to the enhancement of the yield stress of the base material with the strain-rate [4].

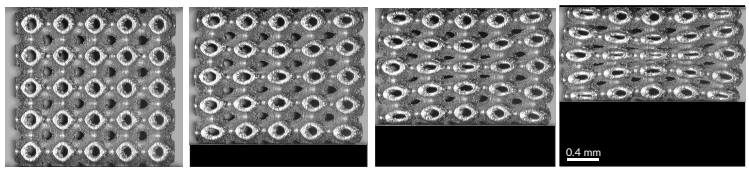

(a) Primitive

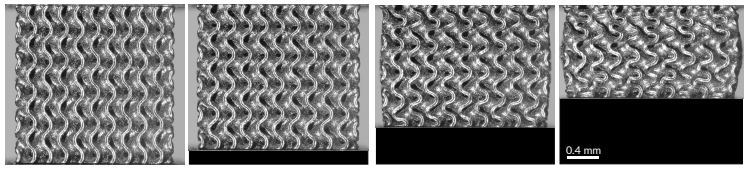

(b) Gyroid Sheet

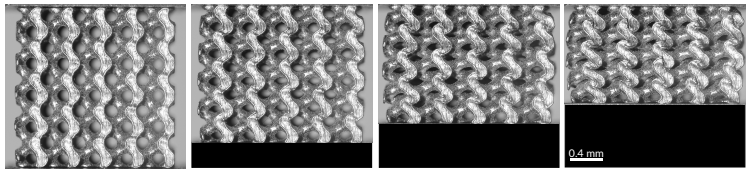

(c) Gyroid Skeletal

FIGURE 4 Pictures of the samples during a quasi-static compression along the X-axis.

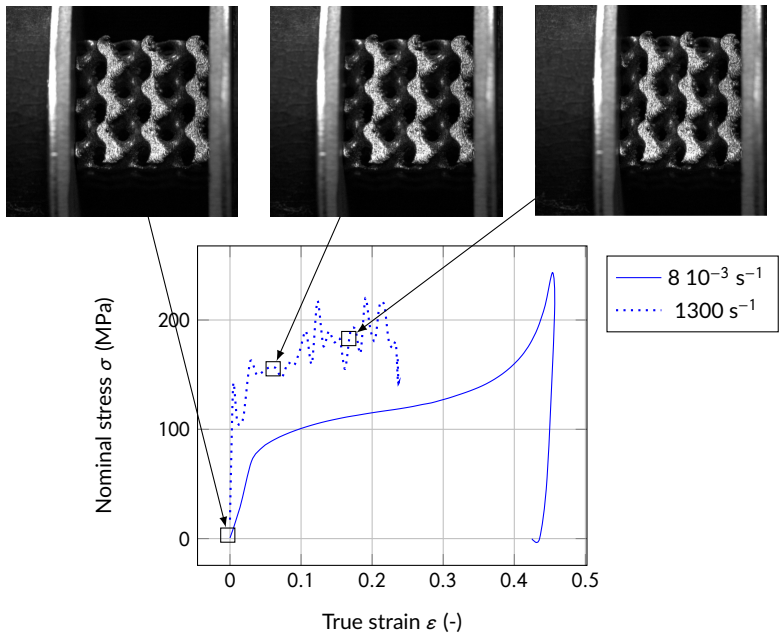

FIGURE 5 Experimental results of compressive tests on Inconel 718 Gyroid skeletal-X in dynamic and quasi-static.

4 | CONCLUSIONS & PERSPECTIVES

In this work, compression tests in quasi-static and dynamic regime have been performed on three different TPMS structures in Inconel 718 alloy obtained by additive manufacturing. The resulting samples presented some differences in the relative density (from 0.32 for the gyroid skeletal to 0.35 for the gyroid sheet). Those differencies where however not sufficient to explain the discrepencies between the material parameters of the three geometries. The local strain mechanisms and more precisely the plastic deformation is the cause of the enhanced behaviour of sheet gyroid in comparison to primitive and skeletal gyroid structures. The latest one displays the largest part on rigid body motion and is thus the one with the smalled SEA. The primitive geometry displayed an anisotric Young's modulus, greater in the X-direction in opposition to the other geometries. Inconel gyroids, both sheet and skeletal geometries, appear to be isotropic in compression. In the future, more local analysis will be pursued to confirm the origin of this anisotropy as well as dynamic loadings with SHPB to complete this study.

References

[1] Ashby MF, Bréchet YJM. Designing hybrid materials. Acta Materialia 2003;51(19):5801–5821.

[2] Brechet Y, Embury JD, Bréchet Y, Embury JD. Architectured materials: Expanding materials space. Scripta Materialia 2013;68(1):1–3. http://dx.doi.org/10.1016/j.scriptamat.2012.07.038.

[3] Hawreliak JA, Lind J, Maddox B, Barham M, Messner M, Barton N, et al. Dynamic Behavior of Engineered Lattice Materials. Scientific Reports 2016;6(December 2015):1–7.

[4] Tancogne-Dejean T, Spierings AB, Mohr D. Additively-manufactured metallic micro-lattice materials for high specific energy absorption under static and dynamic loading. Acta Materialia 2016;116:14–28. http://dx.doi.org/10.1016/j.actamat.2016.05.054.

[5] Tancogne-Dejean T, Mohr D. Stiffness and specific energy absorption of additively-manufactured metallic BCC metamaterials composed of tapered beams. International Journal of Mechanical Sciences 2018;141(February):101–116. https://doi.org/10.1016/j.ijmecsci.2018.03.027.

[6] Cao X, Xiao D, Li Y, Wen W, Zhao T, Chen Z, et al. Dynamic compressive behavior of a modified additively manufactured rhombic dodecahedron 316L stainless steel lattice structure. Thin-Walled Structures 2020;148(June 2019):106586. https://doi.org/10.1016/j.tws.2019.106586.

[7] Li X, Xiao L, Song W. Compressive behavior of selective laser melting printed Gyroid structures under dynamic loading. Additive Manufacturing 2021;46(April):102054. https://doi.org/10.1016/j.addma.2021.102054.

[8] Novak N, Al-Ketan O, Krstulović-Opara L, Rowshan R, Abu Al-Rub RK, Vesenjak M, et al. Quasi-static and dynamic compressive behaviour of sheet TPMS cellular structures. Composite Structures 2021;266(March):1–10.

[9] Al-Ketan O, Abu Al-Rub RK. MSLattice: A free software for generating uniform and graded lattices based on triply periodic minimal surfaces. Material Design and Processing Communications 2021;3(6):1–10.

[10] Bouix R, Viot P, Lataillade JL. Polypropylene foam behaviour under dynamic loadings: Strain rate, density and microstructure effects. International Journal of Impact Engineering 2009;36(2):329–342.

[11] Al-Ketan O, Rowshan R, Abu Al-Rub RK. Topology-mechanical property relationship of 3D printed strut, skeletal, and sheet based periodic metallic cellular materials. Additive Manufacturing 2018;19:167–183. http://dx.doi.org/10.1016/j.addma.2017.12.006.

[12] McKown S, Shen Y, Brookes WK, Sutcliffe CJ, Cantwell WJ, Langdon GS, et al. The quasi-static and blast loading response of lattice structures. International Journal of Impact Engineering 2008;35(8):795–810.

[13] Xiao L, Song W, Wang C, Tang H, Fan Q, Liu N, et al. Mechanical properties of open-cell rhombic dodecahedron titanium alloy lattice structure manufactured using electron beam melting under dynamic loading. International Journal of Impact Engineering 2017;100:75–89. http://dx.doi.org/10.1016/j.ijimpeng.2016.10.006.

[14] Zhang L, Feih S, Daynes S, Chang S, Wang MY, Wei J, et al. Energy absorption characteristics of metallic triply periodic minimal surface sheet structures under compressive loading. Additive Manufacturing 2018;23(July):505–515. https://doi.org/10.1016/j.addma.2018.08.007.